Two-Winding Procedure for the Measurement of the Anhysteretic Curve Points and Small-Signal Magnetic Permeability of Ferromagnetic Materials

# Two-winding procedure for the measurement of the anhysteretic curve points and small-signal magnetic permeability of ferromagnetic materials

Emir Pošković, *Member, IEEE*, Fausto Franchini, Luca Ferraris *Member, IEEE*

***Abstract*— At a first approximation and sufficiently low frequencies, two macroscopic phenomena influence the hysteresis cycle shape in ferromagnetic materials: magnetic hysteresis and magnetic saturation. Different magnetic models use the anhysteretic curve as a fundamental locus in the magnetic material representation. In the literature, many authors proposed easier measurement methods to obtain the anhysteretic curve, or methods, which envisage the use of standard equipment already available on the market. In the present work, a measurement procedure is outlined, involving only two windings, being partly or fully compliant with the sample preparation described in the 60404 standards. Additionally, the proposed method is suitable to measure the small-signal permeability in each point of the anhysteretic curve right after the determination of the point itself. Also, the local magnetic permeability is obtained directly from the measurement. The method is executed on three toroidal samples made of different materials: a laminated sheet, a Soft Magnetic Composite and an amorphous ferrite core. The results are then compared with those of a very low frequency, large cycle conventional measurement, showing a good matching with the expected anhysteretic behavior of the three materials.**

***Index Terms* — Magnetism, magnetic modeling, hysteresis, anhysteretic, magnetic measurements, local magnetic permeability, laminated steel, Soft Magnetic Composite, Ferrites**

## I. INTRODUCTION

The magnetic behavior of the materials characterizes many applications in several industrial sectors, primarily those related to electrical and electronic devices. From this point of view, modelling and predicting magnetic phenomena [1-7] play an important role in the design of various components, such as electrical machines, sensors, inductances etc. [8-13]. For this reason, knowing the magnetic parameters is essential, and it is possible to identify and investigate ferromagnetic materials through magnetic measurement [14-17]. Different methods and equipment are implemented to investigate magnetic properties; the more popular are the Epstein frame, toroid test and single sheet tester (SST) [18-26]. Therefore, the hysteresis cycle represents the starting point for obtaining more information about various ferromagnetic magnetic materials [27-30]. Furthermore, through careful analysis, it is possible to extract from the hysteresis cycle valuable data to model the magnetic behavior [31-34].

At a first approximation and sufficiently low frequencies, two macroscopic phenomena influence the hysteresis cycle shape in ferromagnetic materials: magnetic hysteresis and magnetic saturation.

The representation of the material's magnetic behavior can be split into the same two components. First, the so-called anhysteretic curve depicts the virtual absence of magnetic hysteresis [35]. The anhysteretic curve, in its entirety, has a weak physical meaning: the induction value of a material possibly subjected to magnetic stresses does not follow the anhysteretic curve in any case. Conversely, each one of its points precisely represents an equilibrium state between the internal magnetization and the external magnetic field [36]. Furthermore, each point in the curve shows the same local differential permeability for a variation of the external magnetic field in either direction.

The anhysteretic locus existence is well-known, and its implications are used in many applications and devices, such as magnetic recording. The Jiles-Atherton model of hysteresis and other models use the anhysteretic approach [37],[38]. The anhysteretic curve contains all the information on the saturation phenomenon. Moreover, being a quasi-DC measurement, it is not affected by eddy currents contributions and from the hysteresis itself. Several F.E.M. simulation tools may benefit from an accurate recording of the anhysteretic curve. Despite this, the relative measurement procedures are not optimized and require more time to be performed than the other magnetic characterizations typically regulated by standards.

In the literature, many authors proposed methods for simplification or methods which envisage the use of standard equipment already available on the market [39]. The measurements generally involve closed magnetic circuits, such as toroids or Epstein frames, to reach the highest field uniformity, avoiding any unwanted measurement uncertainty.

The newest methods allow using a standard hysteresigraph by adding to the sample a third winding, through which an additional DC magnetic field can be applied [40].

Another approach involves the sample heating above the Curie temperature in presence of a DC field, which leads to slightly different results [41].

In the present work, a measurement procedure is outlined, involving only two windings, being partly or fully compliant

Paper presented at the 2023 14th International Symposium on Diagnostics for Electrical Machines, Power Electronics and Drives (SDEMPED), August 28-31, Chania, Greece.

E. Pošković, is with the Energy Department, Politecnico di Torino, Torino, 10129, Italy (e-mail: emir.poskovic@polito.it).

F. Franchini, is with the Energy Department, Politecnico di Torino, Alessandria, 15121, Italy (e-mail: fausto.franchini@polito.it).

L. Ferraris, is with the Energy Department, Politecnico di Torino, Alessandria, 15121, Italy (e-mail: luca.ferraris@polito.it).

with the sample preparation described in the IEC 60404 standards.

Additionally, the proposed method can be used to measure the small-signal permeability in each point of the anhysteretic curve right after the determination of the point itself. The peculiarity consists of local magnetic permeability measurement.

Finally, the method is executed on three toroidal samples made of different materials: a laminated sheet [42], a Soft Magnetic Composite (SMC) [43],[44] and an amorphous ferrite core [45],[46]. The results are then compared with those of a very low frequency, large cycle conventional measurement, showing a good matching with the expected anhysteretic behavior of the three materials.

## II. Methods Definition

The measurement procedure of the proposed method consists of different steps are described in detail. Afterwards, the procedure is validated through the tests on the three different magnetic materials, chosen for their hysteresis cycle peculiarities.

### A. *Two-windings, point-by-point measurement procedure*

Several ways are available for measuring the single points of the anhysteretic curve. The proposed method involves a particular magnetization stimulus having a specific shape. This particular stimulus allows the integration of functions in a single primary winding, while in other methods they were implemented with two windings. The total number of windings is then reduced from 3 to 2. In Fig. 1 an example of the common three-windings configuration is showed.

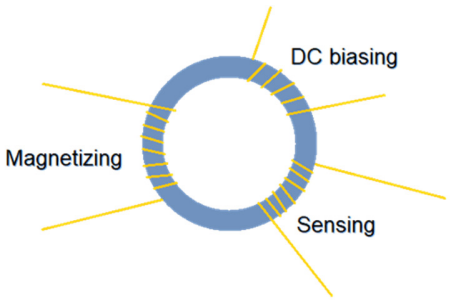


**Fig. 1.** *Three windings approach, as found in the literature*

For the aim of this work, the sample's primary winding is connected to a low noise, high current, DC-coupled power supply (Fig. 2). The proposed method involves a power supply capable of regulating the current waveform, but similar results could be obtained with voltage-controlling power supplies. The main drawback of the current regulation is its intrinsic low speed, which limits the maximum allowable slope due to possible unwanted oscillation. On the other hand, the current regulation allows direct and easy control of the magnetic field waveform.

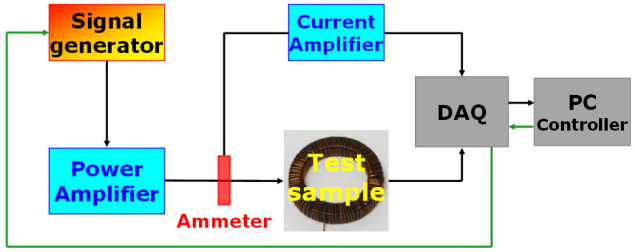


**Fig. 2.** *The measurement system: real-time flux waveform control*

As stated before, a software generator (Labview + NI USB-6211 DAQ board) drives a power supply in current mode (Kikusui PBZ20-20), so the controlled parameter is the current. The applied waveform is composed of five different parts, as shown in Fig. 3:

a. slow current raise until a specified DC value ($i_1$);

b. damped oscillating (of amplitude $i_2$) phase centered on that value, corresponding to the measured point;

c. repeated, small-signal oscillation around the measurement point, also named *holding time;*

d. slow current fall until zero;

e. damped oscillating phase (of amplitude $i_2$) with zero final value.

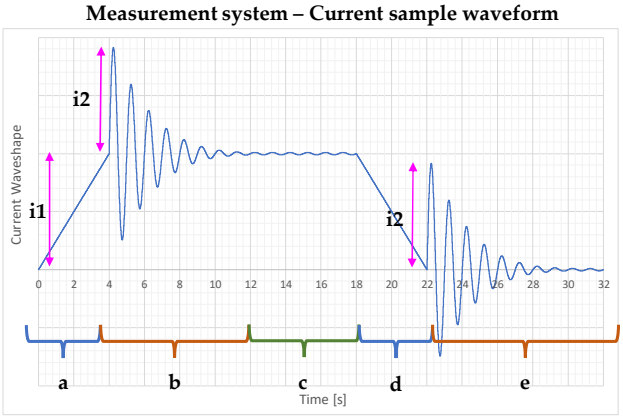


**Fig. 3.** *The measurement system: current waveform*

The damped oscillations act as demagnetization phases. The first demagnetization settles on a non-zero current value (a), so the following curve (b) moves around the point to be measured. The second one (e) is always centered on a zero-final value, thus bringing the material at zero remanence. In fact, the concept of demagnetization also applies to non-zero final current values, with the same general meaning of nulling the remanence relative to the specific current point. All the oscillating envelopes (b, e) are quadratic, instead of linear, thus reaching better demagnetization precision in less time.

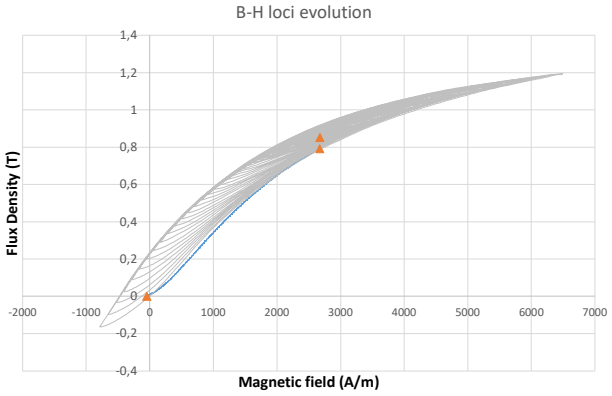


**Fig. 4.** *B-H loci evolution during a single anhysteretic point measurement*

Fig. 4 shows the BH trend during the (a – slow current raise) and (b) phases, which correspond to slow current raise and demagnetization. Three main BH points are visible: the initial demagnetized state in the origin, the end of the first magnetization phase, the final anhysteretic point at the same magnetic field of the previous point.

The anhysteretic curve in then made by many anhysteretic points obtained with the aforementioned method at different final magnetic field levels.

The subsequent small signal oscillation (c) around the last current point (holding time) can be used to extract a measurement of the reversible, small-signal permeability – extending the initial permeability concept also to points other than the origin, as other authors already stated [28].

The reason to fully demagnetize the sample after every point is twofold. Firstly, the final induction value after demagnetization is considered to be null. This can be used to compensate for the measurement drift due to small voltage offsets. A hypothesis, successfully verified during the early tests hereafter presented, is that the integrator drift rate was constant over the whole measurement window. Furthermore, a final zero current has the advantage of limiting the sample temperature. Many current raise and demagnetization phases without returning to the null value could be concatenated to shorten the total measurement time; on the other hand, it could also lead to excessive sample heating.

### *B. Differences with the field-averaging numerical technique*

Contrary to the time-consuming method of real measurement, some numerical systems are available that, although much less precise, can partly estimate the characteristics of the anhysteretic curve.

The field-averaging line method is the most straightforward technique, starting from a single full-cycle measurement. For each induction value, the anhysteretic points are obtained by averaging the magnetic field values of the cycle's ascending and descending portions. As a result, the calculated curve shows a less steep path than the correct anhysteretic curve.

Given the difficulty of establishing reliable and adaptable formulas to effectively represent the behavior of many materials, a possible way to simplify the treatment could consist in analyzing the differences between the measured anhysteretic curve and the mean-field curve. This type of analysis will be the subject of one of the following research paths.

The main purpose of this method is not a correct estimation of the anhysteretic points. Instead, the former can be used as a reference to the analysis of the latter. At different parts of the cycle, the anhysteretic points lie closer to or further away from the B axis than the average curve.

### *C. Quasi-DC hysteresigraph*

The point-by-point anhysteretic curve must be compared with the classical hysteresigraph measurement, here performed with a self-implemented instrument capable of the quasi-DC first magnetization and full hysteresis cycle detection. The previously demagnetized materials undergo a magnetic stimulus with the following structure, as shown in Fig. 5:

- two full cycles at very low frequency (0.25 Hz in the tests of this work);
- a damped oscillation phase for the final demagnetization.

In Fig. 5 the following points are highlighted:

- A: origin of the magnetizing current
- B: first positive peak of the sinusoidal current waveform, from which the hysteresis cycle was recorded
- C: second positive peak of the sinusoidal current waveform, closing the hysteresis loop.

The first quarter of the first full cycle is a direct measurement of the first magnetization curve (from point A to point B), which was not reported in Fig. 6 on purpose to maintain clarity of the zoomed zone. The true full cycle is obtained starting from the first current peak (point B) and ending on the second current peak (point C). The final demagnetization phase has the same resetting effect as in the anhysteretic measurements.

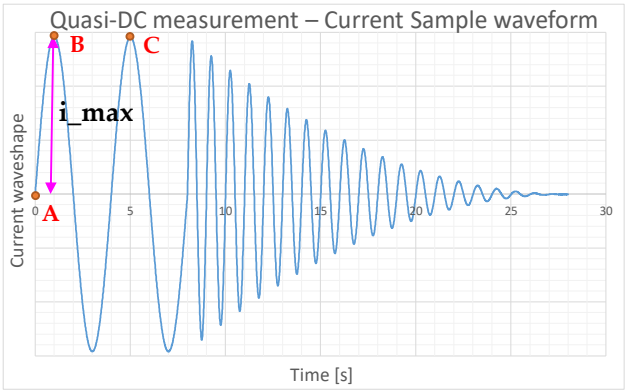


**Fig. 5.** *Sample waveform used for the quasi-DC measurements*

For a better removal of all the measurement offsets, after having subtracted the DC contributions from the current and voltage waveforms, and after the calculation of the flux density waveform, the full-cycle representation was used to a more precise offset cancellation. Since the full-cycle should be centered on the origin, the coercivity and remanence values can be easily stated by averaging the modulus of $+H_c$ and $-H_c$ points and of $+B_r$ and $-B_r$ points, respectively. The so obtained offsets

in Hc and Br can be effectively used for the offset correction of the entire waveform (Fig. 6).

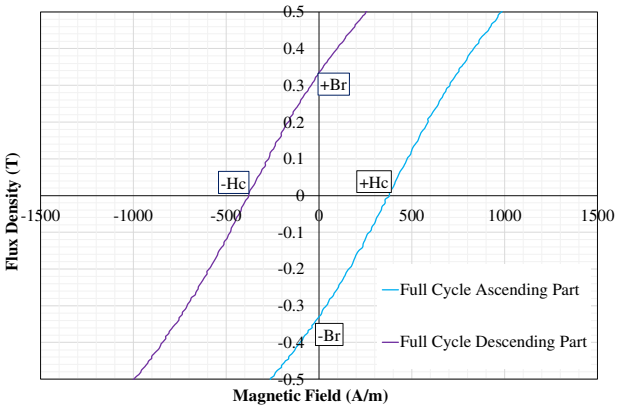


**Fig. 6.** *Full hysteresis cycle close-up (laminated sheet): $B_r$ and $H_c$ values*

### *D. Curve comparison – anhysteretic permeability*

The comparison between the anhysteretic curve and the first magnetization curve shows that, in the former, the Rayleigh zone is absent: the relative permeability near the origin is similar to or even greater than the maximum relative permeability classically calculated. The concept of anhysteretic permeability can be defined similarly to conventional permeability, but built on the anhysteretic curve instead of the first magnetization curve. For every magnetization state, the anhysteretic permeability is assumed to be equal or greater than the conventional one.

This behavior can be observed in detail in the figures of Section IV.

### *E. Small-signal permeability measurements*

The small-signal permeability represents the extension of the Rayleigh zone concept to the whole BH space. The small-signal permeability is thus defined only for small field changes around a specified point, and similarly to the initial permeability is lower than the maximum in the same point.

The small-signal permeability measurements were taken thanks to the test phase named holding time. During that phase the measuring system holds the current DC value constant. This constant value is summed to a very low-level sinusoidal current waveform; the oscillation amplitude, frequency and duration can be set in the setup panel.

A high number of small, local hysteresis cycles was recorded during this phase. Due to the very low amplitude of the oscillating component, the signal-to-noise ratio was rather poor and had to be enhanced through a synchronous filtering routine to correctly measure the average induction level and the small-signal permeability.

The average induction level is recorded as the induction of the anhysteretic curve [47], and it is paired with the magnetic field value obtained from the average current level. The small-signal permeability is then computed with a further linear interpolation of the filtered small-signal cycle, so that only the conventional relative permeability is measured, without splitting it in the real and imaginary parts. The induction measurement drift in the holding phase is low enough to guarantee an adequate precision of the average inductance level, but it is too wide to allow a precise complex permeability computation.

## III. SELECTED MATERIALS

For the purposes of the present work, the proposed method is applied to three different materials in toroidal form (Fig. 7):

- a non-grain-oriented commercial laminated sheet
- a self-prepared SMC core with an organic layer (epoxy resin content 0.2 wt.%)
- a commercial amorphous ferrite core for EMI filtering.

They were chosen because of the strong differences that exist between them in terms of composition and microstructure, and, consequently, also in terms of magnetic properties. The laminated sheet toroid is composed by several insulated sheets piled in a stack, while the other two samples are homogeneous and isotropic through the entire volume. Being commercial items, the amorphous sample and the laminated stack slightly differ in size from the standard 60404 specifications. The dimensions data of the proposed specimen are reported in TABLE I.

**Fig. 7.** *The three measured toroidal samples (laminated, SMC, amorphous)*

The laminated stack owns all the properties of a common laminated core: high maximum permeability, far saturation, and good energetic behaviors until 1 kHz. As expected, the SMC ring shows a lower permeability value, which is supposed to be more stable over frequency, and a reduced but still high saturation induction. The amorphous core has the earlies saturation, a very stable permeability over frequency, and a very low coercive field.

TABLE I. SAMPLE DIMENSIONS AND COIL TURN NUMBERS

| | ***Laminated stack*** | ***SMC*** | ***Amorphous*** |
|---|---|---|---|
| **Thickness [mm]** | 4.7 | 5.22 | 7.45 |
| **Outer Diameter [mm]** | 30 | 40.09 | 28.98 |
| **Inner Diameter [mm]** | 20 | 30.12 | 19.32 |
| **Weight [g]** | 13.7 | 20.98 | 13.1 |
| **Primary winding turns** | 100 | 73 | 40 |
| **Secondary winding turns** | 20 | 25 | 23 |

## IV. RESULTS

A graphical full-cycle comparison of the three materials is first introduced to highlight the difference between them in terms of cycle area, remanence, and saturation induction (Fig. 8). The data are related to the quasi-DC tests. As expected, the results comply with the results in the literature, which are obtained through other methods. The advantages of the proposed technique are mainly in the simpler circuit and in the single excitation winding topology.

The complete data set of each material is then presented, consisting of the anhysteretic curve points, the first magnetization and the ascending and descending parts of the cycle. The anhysteretic curve of the three sample materials is expected to be closer to the vertical axis than the curve calculated by averaging the field values. The results confirm this behavior for all the analyzed materials. Furthermore, the scale of the vertical axis is maintained constant for all proposed materials. Considerations are made about the comparison between the anhysteretic measurement and the average field line, represented with the green line in the following graphs of Fig. 9, Fig. 12 and Fig. 15.

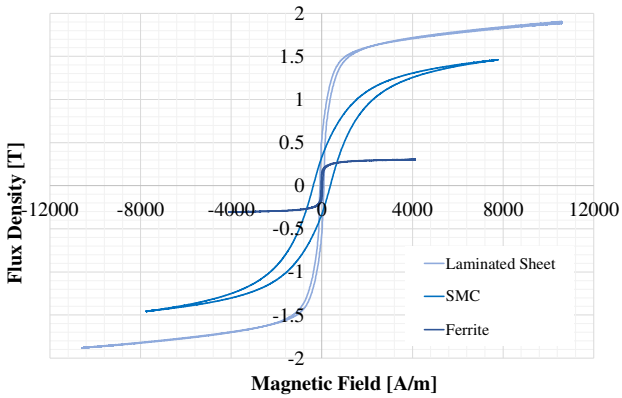


**Fig. 8.** *The hysteresis cycles from the quasi-DC tests*

The anhysteretic measurements were stopped at lower levels with respect to the full-cycle recordings, to avoid sample overheating. To reach a specified anhysteretic point, the maximum current would go at a much higher peak value due to the presence of the demagnetizing phase. Furthermore, the most relevant range for an adequate comparison between the different curves is the central part of the cycle, since, during saturation, the anhysteretic curve and the full cycle become very close to each other.

The anhysteretic curve doesn't represent the real magnetization characteristics of the material, especially at low magnetic field conditions. Conversely, the first magnetization does represent exactly such behavior.

### A. *Laminated stack*

The laminated stack has the highest permeability and saturation induction, together with a low remanence. The anhysteretic curve shows a pronounced deviation from the average field line (Fig. 9), with an even steeper anhysteretic permeability near the origin (Fig. 10). This behavior is typical of the bulk (not made of powders) materials with high permeability. The small-signal permeability is shown in Fig. 11; the initial value is high and remains around 100 at 1000 A/m. The small-signal magnetic permeability reached almost constant values between 20-30 for higher magnetic fields.

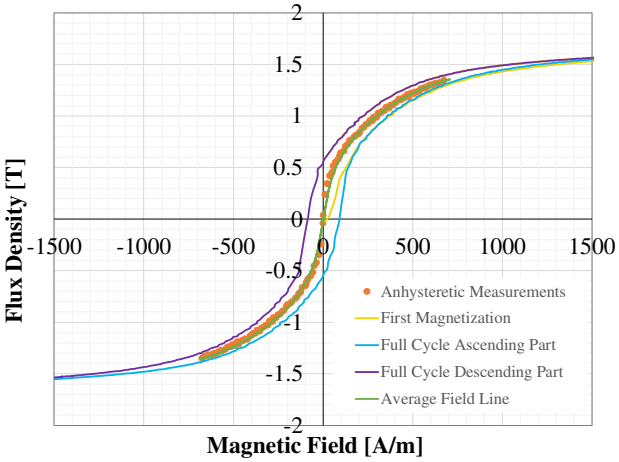


**Fig. 9.** *Full cycle and anhysteretic data – laminated sample*

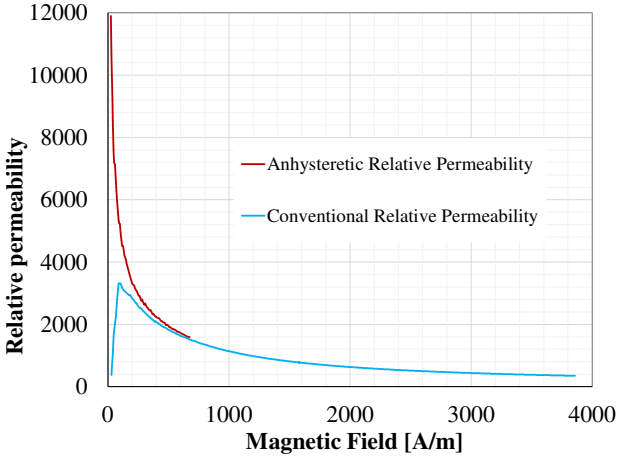


**Fig. 10.** *Anhysteretic and conventional permeability – laminated sample*

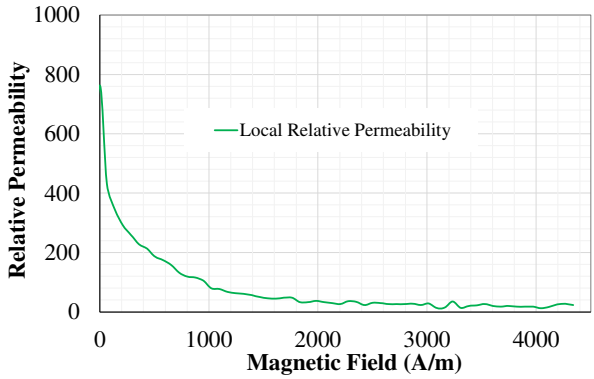


**Fig. 11.** *Small-signal permeability - laminated sample*

### B. *SMC*

The SMC ring shows a reduced permeability, a smoother cycle and an earlier saturation. Compared to the laminated material, the SMC sample shows a much higher coercivity,

while retaining a similar remanence value. The anhysteretic points are placed near the average field line (Fig. 12), which is a common behavior of SMC materials. Consequently, the anhysteretic permeability divergence is less pronounced (Fig. 13). In Fig. 14, the small-signal permeability of the SMC specimen is shown. The initial magnetic permeability, a value of 106, is lower than the laminated steel one. On the other hand, the values at high magnetic fields are slightly higher compared to electrical sheets. The saturation is slower and has not reached the level of completion like for other tested materials. Therefore, the small-signal magnetic permeability reduction is lowly emphasized with the increment of the magnetic field and can be attractive for DC bias current properties.

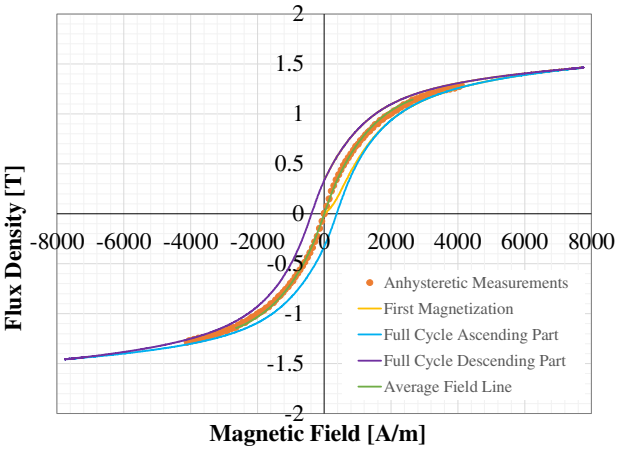


**Fig. 12.** *Full cycle and anhysteretic data – SMC sample*

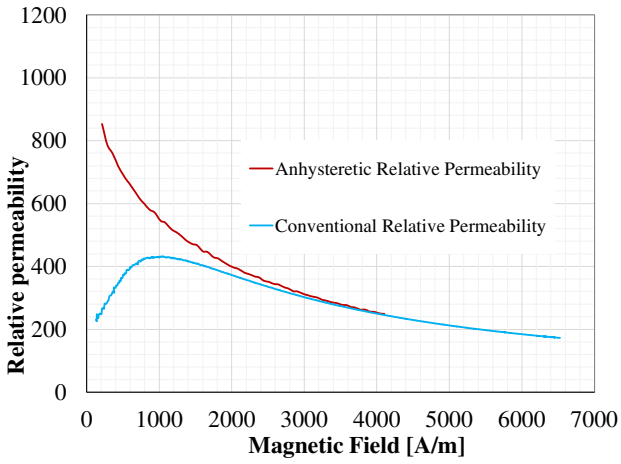


**Fig. 13.** *Anhysteretic and conventional permeability – SMC sample*

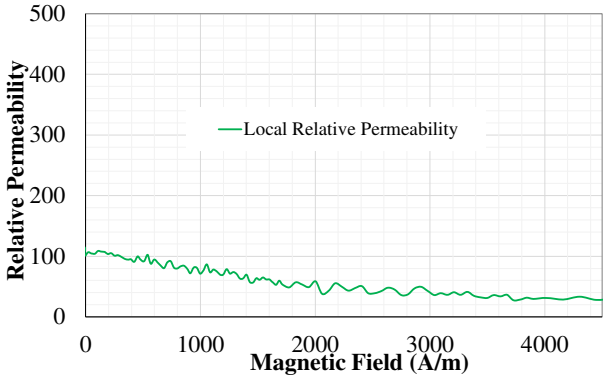


**Fig. 14.** *Small-signal permeability - SMC sample*

### *C. Amorphous core*

The amorphous ring shows a high maximum permeability, comparable with the laminated sheet, and the earliest saturation. Compared to the laminated material, the amorphous material shows reduced remanence and a very low coercivity value. Due to the small cycle area, the ascending and descending parts of the cycle are very close to each other (Fig. 15). Despite this, the anhysteretic measurements show a low noise content and a behavior compliant with the expected material properties: an average between the last two cases (Fig. 16). The small-signal magnetic permeability for the amorphous sample is shown in Fig. 17. The initial magnetic permeability shows a high value, which is typical for ferrite materials. Also, the small-signal permeability values at high magnetic fields are almost zero. This result confirms the early saturation of the ferrite materials.

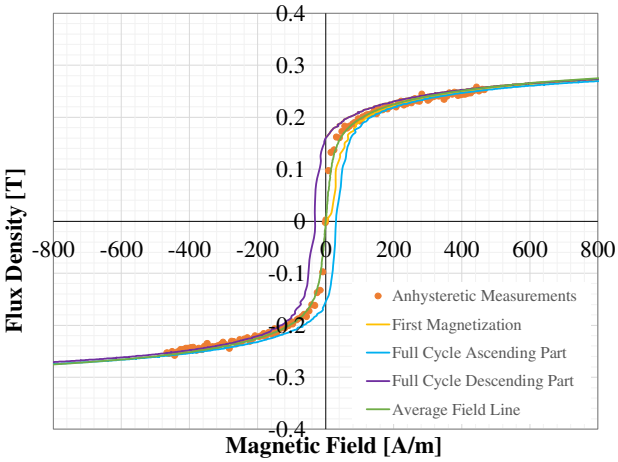


**Fig. 15.** *Full cycle and anhysteretic data – amorphous sample*

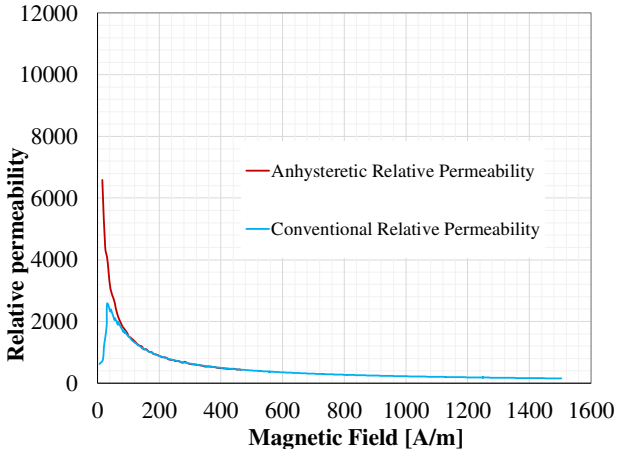


**Fig. 16.** *Anhysteretic and conventional permeability – amorphous sample*

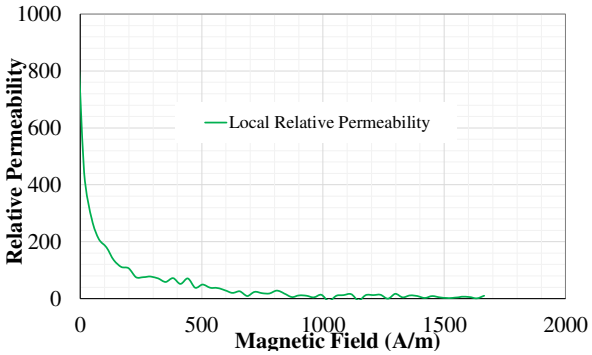


**Fig. 17.** *Small-signal permeability - amorphous sample*

## V. CONCLUSIONS

The present work demonstrates the availability of a simple method to perform anhysteretic measurements with a two-winding configuration, which is compliant with the 60404 standard specifications for the sample preparation. Also, the small-signal magnetic permeability has been measured.

The proposed method was applied to three toroidal samples made of different materials. The results highlight the peculiarities and the difference between the three measured materials, supporting the method's validity.

Many future research paths emerge from the present work, including: the full data analysis and small-signal permeability varying the frequency; the analysis and the modeling of the conventional/anhysteretic relative permeability ratio; the application of the anhysteretic measurements obtained with the proposed method to the Jiles-Atherton model. Moreover, other materials will be investigated [48],[49]. The correct assessment of the small-signal permeability can be helpful for a detailed analysis of the DC bias behavior of several magnetic materials.

## ACKNOWLEDGMENT

The part of the research activities developed by Emir Pošković was carried out within the framework of Ministerial Decree no. 1062/2021 and received funding from the FSE REACT-EU - PON Ricerca e Innovazione 2014-2020. This manuscript reflects only the views and opinions of the authors, neither the European Union nor the European Commission can be considered responsible for them.

## REFERENCES

[1] A. Krings, J. Soulard, "Overview and Comparison of Iron Loss Models for Electrical Machines", in *J. of Electrical Engineering*, vol. 10 (3), 2010.

[2] J. Takács, "A phenomenological mathematical model of hysteresis," *COMPEL - The international journal for computation and mathematics in electrical and electronic engineering*, Vol. 20 (4), pp. 1002-1015, 2001.

[3] M. Popescu, D. M. Ionel, A. Boglietti, A. Cavagnino, C. Cossar and M. I. McGilp, "A General Model for Estimating the Laminated Steel Losses Under PWM Voltage Supply," in *IEEE Transactions on Industry Applications*, vol. 46 (4), pp. 1389-1396, July-Aug. 2010.

[4] Z. Ye, "Modelling and experimental analysis of core losses of SMC components," *World PM2014 Congress*, Orlando (USA), 18÷22 May 2014, Conf. Proc. pp. 228–231.

[5] S. Yanase, H. Kimata, Y. Okazaki and S. Hashi, "A simple predicting method for magnetic losses of electrical steel sheets under arbitrary induction waveform," in *IEEE Transactions on Magnetics*, vol. 41 (11), pp. 4365-4367, Nov. 2005.

[6] M. S. Lancarotte and A. de A. Penteado, "Estimation of core losses under sinusoidal or non-sinusoidal induction by analysis of magnetization rate," in *IEEE Transactions on Energy Conversion*, vol. 16, (2), pp. 174-179, June 2001.

[7] I. T. Gürbüz, P. Rasilo, F. Martin, O. Osemwinyen and A. Belahcen, "2-D Analytical Model for Computing Eddy-Current Loss in Nonlinear Thick Steel Laminations," in *IEEE Transactions on Magnetics*, vol. 58 (9), pp. 1-4, Sept. 2022.

[8] A. Krings, M. Cossale, A. Tenconi, J. Soulard, A. Cavagnino, A. Boglietti, "Magnetic materials used in electrical machines", *IEEE Industry Applications Magazine*, pp. 21–28, November/December 2017.

[9] Jian Guo Zhu and You Guang Guo, "Study with magnetic property measurement of soft magnetic composite material and its application in electrical machines,"*2004. IAS Annual Meeting*., Seattle (USA), 3÷7 October 2004, Conf. Proc..

[10] B. Han, X. Liu, Z. Huang, X. Zhang and Y. Zhou, "Loss Calculation, Thermal Analysis, and Measurement of Magnetically Suspended PM Machine," in *IEEE Transactions on Industrial Electronics*, vol. 65 (6), pp. 4514-4523, June 2018.

[11] T. Sato, S. Aya, H. Igarashi, M. Suzuki, Y. Iwasaki and K. Kawano, "Loss Computation of Soft Magnetic Composite Inductors Based on Interpolated Scalar Magnetic Property," in *IEEE Transactions on Magnetics*, vol. 51 (3), pp. 1-4, March 2015.

[12] G. Di Capua, N. Femia, K. Stoyka, "Switching Power Supplies with Ferrite Inductors in Sustainable Saturation Operation," *International Journal of Electrical Power & Energy Systems*, Vol. 93, pp. 494-505, 2017.

[13] S. Vaschetto, Z. Gmyrek, C. Dobler, G. Bramerdorfer and A. Cavagnino, "Experimental Assessment and Modeling of Losses in Interlocked Magnetic Cores," in *IEEE Transactions on Industry Applications*, vol. 58 (4), pp. 4450-4460, July-Aug. 2022.

[14] A. J. Hanson, J. A. Belk, S. Lim, C. R. Sullivan and D. J. Perreault, "Measurements and Performance Factor Comparisons of Magnetic Materials at High Frequency," in *IEEE Transactions on Power Electronics*, vol. 31 (11), pp. 7909-7925, Nov. 2016,

[15] D. Gumbleton-Wood, G. J. Atkinson and L. Sjöberg, "Electromagnetic Properties of Soft Magnetic Composites and Electrical Steels at High Frequencies Considering Material Manufacturing Techniques," *2019 IEEE IEMDC Conf.*, San Diego (USA), 12÷15 May 2019, Conf. Proc. pp. 2027-2034.

[16] J. H. J. Potgieter, F. J. Márquez-Fernández, A. G. Fraser and M. D. McCulloch, "Effects Observed in the Characterization of Soft Magnetic Composite for High Frequency, High Flux Density Applications," in *IEEE Transactions on Industrial Electronics*, vol. 64, (3), pp. 2486-2493, March 2017.

[17] Z. Gmyrek, M. Strąkowska, B. Więcek, "A method of local magnetic loss determination in punched ferromagnetic strips," in *Journal of Magnetism and Magnetic Materials*, Vol. 355, pp. 282-288, 2014.

[18] S. Tumanski., "Magnetic Materials from: Handbook of Magnetic Measurements", CRC Press, 23 June 2011.

[19] Y. Zhang, N. Alatawneh, M. C. Cheng and P. Pillay, "Magnetic core losses measurement instrumentations and a dynamic hysteresis loss model," *2009 IEEE EPEC Conf.*, Montreal (Canada), 22÷23 October 2009, Conf. Proc. pp. 1-5.

[20] M. J. Manyage and P. Pillay, "New Epstein Frame for Core Loss Measurements at High Frequencies and High Flux Densities," *2008 IEEE IAS Annual Meeting*, Edmonton, (Canada), 5÷9 October2008, Conf. Proc. pp. 1-6.

[21] D. Miyagi, T. Yamazaki, D. Otome, M. Nakano and N. Takahashi, "Development of Measurement System of Magnetic Properties at High Flux Density Using Novel Single-Sheet Tester," in *IEEE Transactions on Magnetics*, vol. 45 (10), pp. 3889-3892, Oct. 2009.

[22] E. Pošković, F. Franchini, L. Ferraris, F. Carosio, M. Actis Grande, "Rapid Characterization Method for SMC Materials for a Preliminary Selection", *MDPI. Appl. Sci.*, vol. 11 (24), December 2021.

[23] Z. Gmyrek, "Single Sheet Tester With Variable Dimensions," in *IEEE Trans. Instrum. Meas.*, vol. 65 (7), pp. 1661-1668, July 2016.

[24] J.G. Zhu, J.J. Zhong, V.S. Ramsden, Y.G. Guo, "Power losses of soft magnetic composite materials under two-dimensional excitation," in *AIP J Appl Phys.*, 85(8), pp.4403–4405, 1999.

[25] Y. Li, Y. Liu, F. Liu, Q. Yang and P. Ren, "Magnetic Anisotropic Properties Measurement and Analysis of the Soft Magnetic Composite Materials," in *IEEE Transactions on Applied Superconductivity*, vol. 24 (5), pp. 1-4, Oct. 2014.

[26] A. R. Asari, Y. Guo and J. Zhu, "Measurement of magnetic properties of soft magnetic composite material (SOMALOY 700) by using 3-D magnetic tester," *2016 IEEE ICEMS Conf.*, Chiba (Japan), 13÷16 November 2016, Conf. Proc. pp. 1-5.

[27] W. Xu, N. Duan, S. Wang, Y. Guo and J. Zhu, "Modeling and Measurement of Magnetic Hysteresis of Soft Magnetic Composite Materials Under Different Magnetizations," in *IEEE Transactions on Industrial Electronics*, vol. 64 (3), pp. 2459-2467, March 2017.

[28] Zuzana Birčáková, Peter Kollár, Miloš Jakubčin, Ján Füzer, Radovan Bureš, Mária Fáberová, "Reversible and irreversible magnetization processes along DC hysteresis loops of Fe-based composite materials," in *Journal of Magnetism and Magnetic Materials*, Volume 483, pp. 183-190, 2019.

[29] B. Jankowski, B. Slusarek, J. Szczygłowski, K. Chwastek, "Modelling Hysteresis Loops in Fe-Based Soft Magnetic Composites Using Takács Description,"in *Acta Physica Polonica A*, Vol. 128 (1), pp. 116-119, 2015.

[30] Dianhai Zhang, Ziyan Ren and C. -S. Koh, "Hysteresis modeling of anisotropic and isotropic bonded NdFeB PM utilizing the Jiles-Atherton hysteresis model," *2013 IEEE ICEMS Conf.*, Busan (South Korea), 26÷29 October 2013, Conf. Proc. pp. 864-867.

[31] Fausto Fiorillo, Carlo Appino, Massimo Pasquale, "Chapter 1 - Hysteresis in Magnetic Materials" from The Science of Hysteresis, Editor(s): Giorgio Bertotti, Isaak D. Mayergoyz, Academic Press, pp. 1-190, 2006.

[32] Zuzana Birčáková, Peter Kollár, Ján Füzer, Radovan Bureš, Mária Fáberová, "Analytical expression for initial magnetization curve of Fe-based soft magnetic composite material,", in *Journal of Magnetism and Magnetic Materials*, Vol. 423, pp. 140-144, 2017.

[33] Peter Kollár, Denisa Olekšáková, Vladimír Vojtek, Ján Füzer, Mária Fáberová, Radovan Bureš, "Steinmetz law for ac magnetized iron-phenolformaldehyde resin soft magnetic composites,", in *Journal of Magnetism and Magnetic Materials*, Vol. 424, pp. 245-250, 2017.

[34] G. Bertotti, "General properties of power losses in soft ferromagnetic materials," in *IEEE Transactions on Magnetics*, vol. 24 (1), pp. 621-630, Jan. 1988.

[35] D. C. Jiles and D. L. Atherton, "Theory of ferromagnetic hysteresis", in *Journal of Magnetism and Magnetic Materials*, vol. 61, pp. 48–60, 1986.

[36] J. M. Silveyra and J. M. Conde Garrido, "On the anhysteretic magnetization of soft magnetic materials", in *AIP Advances* 12, 035019, 2022.

[37] B. Kvasnica and F. Kundracík, "Fitting experimental anhysteretic curves of ferromagnetic materials and investigation of the effect of temperature and tensile strenght", in *Journal of Magnetism and Magnetic Materials*, vol. 162, pp. 43–49, 1996.

[38] J. M. Silveyra and J. M. Conde Garrido, "On the modelling of anhysteretic magnetization of homogeneous soft magnetic materials", in *Journal of Magnetism and Magnetic Materials*, vol. 540, 168430, 2021.

[39] M. Nowicki, "Anhysteretic magnetization measurement methods for soft magnetic materials", in *MDPI Materials*, 11, 2021, 2018.

[40] M. Nowicki, R. Szewczyk and P. Nowak, "Experimental verification of isotropic and anisotropic anhysteretic magnetization models", in *MDPI Materials*, 12, 1549, 2019.

[41] J. Pearson, P. T. Squire and D. Atkinson, "Which anhysteretic magnetization curve?", in *IEEE Transactions on magnetics*, vol. 33, pp. 3970–3972, september1997.

[42] J Sievert, "The measurement of magnetic properties of electrical sheet steel – survey on methods and situation of standards," in *Journal of Magnetism and Magnetic Materials*, Vol. 215–216, pp. 647-651, 2000.

[43] E. Pošković, F. Franchini, L. Ferraris, E. Fracchia, J. Bidulska, F. Carosio, R. Bidulsky, M. Actis Grande, "Recent Advances in Multi-Functional Coatings for Soft Magnetic Composites", *MDPI Materials*, vol. 14 (22), November 2021.

[44] M. De Wulf, L. Anestiev, L. Dupré, L. Froyen, J. Melkebeek, "Magnetic properties and loss separation in iron powder soft magnetic composite materials," in *AIP J. Appl. Phys.*, 91, 7845, 2002.

[45] M. Sugimoto, "The past, present, and future of ferrites," *J. Amer. Ceram. Soc.*, vol. 82, pp. 269–280, 1999.

[46] Raúl Valenzuela, "Novel Applications of Ferrites," in *Physics Research International*, vol. 2012, Article ID 591839, pp. 1-9, 2012.

[47] E. Pošković, F. Franchini, L. Ferraris, "Two-winding procedure for the measurement of the anhysteretic curve points of ferromagnetic materials," *IEEE SDEMPED Conf.*, Chania (Greece), 28÷31 August 2023, pp. 351-356.

[48] H. Tiismus, A. Kallaste, A. Belahcen, T. Vaimann, A. Rassõlkin, and D. Lukichev, "Hysteresis Measurements and Numerical Losses Segregation of Additively Manufactured Silicon Steel for 3D Printing Electrical Machines," in *MDPI Applied Sciences*, vol. 10 (18), p. 6515, Sep. 2020.

[49] S. Wang, Y. Liang, B. Chen, F. Ye, and J. Lin, "AC Iron Loss Prediction and Magnetic Properties of Fe-6.5 wt. % Si Ribbons Prepared by Melt-Spinning," in *MDPI Metals*, vol. 8 (4), p. 259, Apr. 2018.


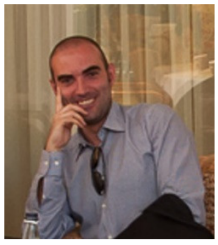

**Emir Pošković** (Member, IEEE) Emir Pošković was born in Sarajevo in Bosnia and Herzegovina, He studied and graduated from the Polytechnic of Turin, where he received B.S. and M.Sc. degree in electrical engineering in 2006 and in 2008, respectively. Also, he received a doctor's degree in electrical energy engineering from the University of Padova in 2020.

He is an Assistant Professor with the Energy Department "G. Ferraris", Politecnico di Torino and a Key Researcher for the Magnetic Characterization Laboratory, Alessandria campus of Politecnico di Torino. His special fields of interest included soft and hard magnetic materials, electrical machines, alternative and renewable energy (micro-hydro, fuel cell, PV-photovoltaic). He has published about 80 scientific papers in conference proceedings and technical journals.

Dr. Poskovic was a recipient of two Best Paper Awards. He is a reviewer for several international journals and conferences.

**Fausto Franchini** received the B.S. degree in electrical engineering from the Politecnico di Torino, Alessandria, Italy, in 2003. Since 2004, he has been a Technician with the Electrical Engineering Laboratory, Politecnico di Torino, where he has been responsible of the laboratory since 2007. His fields of interest include electromagnetic metrology, electromagnetic compatibility, data acquisition, control, and automation.

**Luca Ferraris** received the M.S. degree in electrical engineering from the Politecnico di Torino, Turin, Italy, in 1992. In 1995, he joined the Department of Electrical Engineering (now the Energy Department), Politecnico di Torino, where he is currently an Associate Professor of Electrical Machines and Drives and coordinates the experimental activities of the Electric and Electromagnetic Laboratories. He also leads the activities of the Magnetic characterization Laboratory in the Alessandria campus.

He has published more than 150 technical papers in conference proceedings and technical journals. His research interests are the energetic behavior of machines, innovative magnetic materials for electromagnetic devices, electrical traction, electromagnetic compatibility, and renewable energies.